

# NLO predictions for $t\bar{t}b\bar{b}$ production in association with a light-jet at the LHC

Federico Buccioni

in collaboration with

S. Pozzorini

M. Zoller



Universität  
Zürich <sup>UZH</sup>



FONDS NATIONAL SUISSE  
SCHWEIZERISCHER NATIONALFONDS  
FONDO NAZIONALE SVIZZERO  
SWISS NATIONAL SCIENCE FOUNDATION

## LoopFest XVII



MICHIGAN STATE  
UNIVERSITY

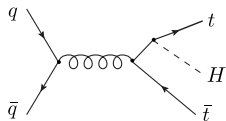
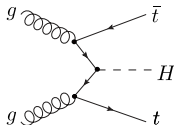
# Outline

- ▶  $pp \rightarrow t\bar{t}H(H \rightarrow b\bar{b})$  at the LHC
- ▶ Open questions in theory predictions for  $t\bar{t} + b$ -jets production
- ▶ Scale choice and large NLO  $K$ -factor in  $pp \rightarrow t\bar{t}b\bar{b}$
- ▶ NLO QCD predictions for  $pp \rightarrow t\bar{t}b\bar{b}j$

# $pp \rightarrow t\bar{t}H (H \rightarrow b\bar{b})$ at the LHC

The determination of the Higgs boson coupling to the top quark is a crucial test of the SM  
top quark Yukawa coupling can be determined through measurements of

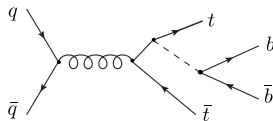
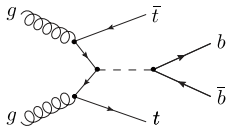
$t\bar{t}H$  associated production



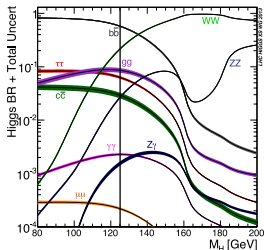
# $pp \rightarrow t\bar{t}H (H \rightarrow b\bar{b})$ at the LHC

The determination of the Higgs boson coupling to the top quark is a crucial test of the SM  
top quark Yukawa coupling can be determined through measurements of

$t\bar{t}H$  associated production



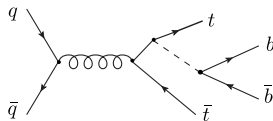
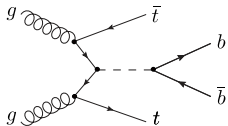
$H$  branching ratio is dominated by  $H \rightarrow b\bar{b}$  decay: channel with highest statistics



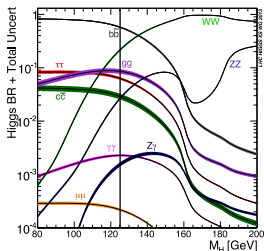
# $pp \rightarrow t\bar{t}H(H \rightarrow b\bar{b})$ at the LHC

The determination of the Higgs boson coupling to the top quark is a crucial test of the SM  
 top quark Yukawa coupling can be determined through measurements of

$t\bar{t}H$  associated production



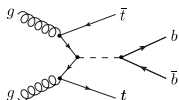
$H$  branching ratio is dominated by  $H \rightarrow b\bar{b}$  decay: channel with highest statistics



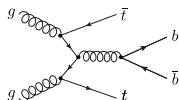
But: this channel suffers from a **large, irreducible QCD background**

$pp \rightarrow t\bar{t} + b$ -jets production

signal



background

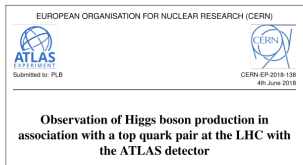


An accurate understanding and description of the background is mandatory for the sensitivity of  $t\bar{t}H(H \rightarrow b\bar{b})$  analyses

# $t\bar{t}H$ discovery at the LHC

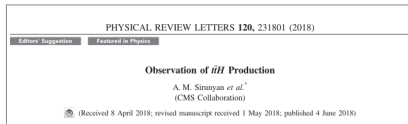
Higgs boson mass measured precisely:  $125.09 \pm 0.24$  GeV

⇒ focus on **Higgs couplings**



6.3 std. dev.

5.2 std. dev.



$t\bar{t}H$  discovery at the LHC  
see talks from W.C. Fisher and M.Liu


# $t\bar{t}H$ discovery at the LHC

Higgs boson mass measured precisely:  $125.09 \pm 0.24$  GeV


⇒ focus on **Higgs couplings**

$t\bar{t}H$  discovery at the LHC  
see talks from W.C. Fisher and M.Liu

EUROPEAN ORGANISATION FOR NUCLEAR RESEARCH (CERN)



Submitted to: P.L.B.



CERN-EP-2018-138  
4th June 2018

**Observation of Higgs boson production in association with a top quark pair at the LHC with the ATLAS detector**

6.3 std. dev.  
5.2 std. dev.

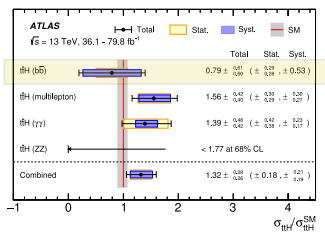
PHYSICAL REVIEW LETTERS **120**, 231801 (2018)

Editors' Suggestion    Featured in Physics

**Observation of  $t\bar{t}H$  Production**

A. M. Sirunyan *et al.*<sup>1</sup>  
(CMS Collaboration)

(Received 8 April 2018; revised manuscript received 1 May 2018; published 4 June 2018)



dominated by systematics

Uncertainty source	$\Delta\sigma_{t\bar{t}H} / \sigma_{t\bar{t}H}$ [%]
Theory uncertainties (modelling)	11.9
$t\bar{t}$ + heavy $f$ flavour	9.9
$t\bar{t}H$	6.0
Non- $t\bar{t}H$ Higgs boson production modes	1.5
Other background processes	2.2
Experimental uncertainties	9.3
Fake leptons	5.2
Jets, $E_{miss}$	4.9
Electrons, photons	3.2
Luminosity	3.0
$\tau$ -lepton	2.5
Flavour tagging	1.8
MC statistical uncertainties	4.4

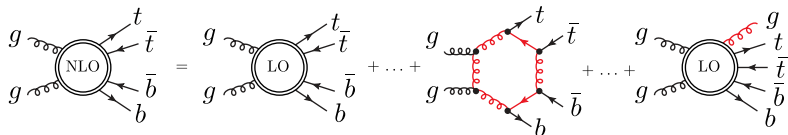
uncertainty dominated by  
 $t\bar{t}$  + heavy flavour modelling in the  $H \rightarrow b\bar{b}$  analyses

# State of the art for $t\bar{t}b\bar{b}$ predictions

- ▶ **First fixed order NLO QCD predictions** for  $pp \rightarrow t\bar{t}b\bar{b}$  [Bredenstein et al. '09, Bevilacqua et al. '09]  
first estimate of theory uncertainties + first NLO calculation for  $2 \rightarrow 4$
- ▶ **First NLOPS simulation** for  $t\bar{t}b\bar{b}$  production in **Powhe1** [Garzelli et al. '13]  
ME in the 5F scheme ( $m_b = 0$ ) + Powheg matching for the parton shower  
since recently available also in the 4F scheme [Bevilacqua et al. '17]
- ▶ **NLOPS generator** for  $t\bar{t}b\bar{b}$  with massive  $b$ -quark in **OpenLoops+Sherpa** [Cascioli et al. '14]  
OpenLoops for 1-loop automation + Sherpa employing MC@NLO matching
- ▶ **NLOPS generator** for  $t\bar{t} + b$ -jet production in 4F scheme in **OpenLoops+Powheg** [Ježo et al. '18]  
OpenLoops for amplitudes automation + Powheg matching in Powheg-Box-Res  
**thorough investigation of uncertainties** related to matching method  
and parton shower modelling
- ▶  $t\bar{t} + b$ -jets simulations in the 4F scheme also available in  
**MG5\_aMC@NLO** [Alwall et al. '14] and **Matchbox** [Plaetzer, Reuschle et al.]



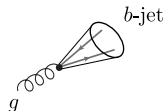
# $t\bar{t} + b$ -jets production in the 4F scheme



We work in the **4F** scheme:  $b$ -quarks are treated as **massive**

⇒ calculation of the ME can be extended to the entire the phase space

⇒ no singularities in  $g \rightarrow b\bar{b}$  splittings. Safe collinear regime with  $g \rightarrow b$ -jet



**On the other hand:**

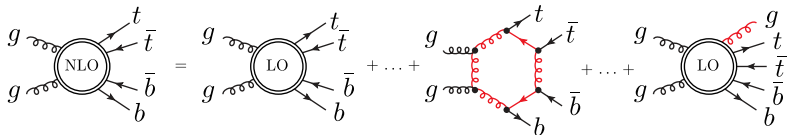
× non-trivial multi-scale multi-particle QCD process

× large scales separation between  $t\bar{t}$  and  $b\bar{b}$  systems

$m_b \sim 5$  GeV       $t\bar{t}$  typical scale up to  $\sim 500$  GeV

**scale choice and estimation of theoretical uncertainties non trivial**

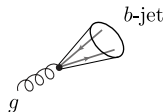
# $t\bar{t} + b$ -jets production in the 4F scheme



We work in the **4F** scheme:  $b$ -quarks are treated as **massive**

⇒ calculation of the ME can be extended to the entire the phase space

⇒ no singularities in  $g \rightarrow b\bar{b}$  splittings. Safe collinear regime with  $g \rightarrow b$ -jet



**On the other hand:**

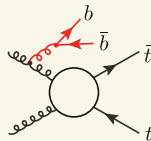
× non-trivial multi-scale multi-particle QCD process

× large scales separation between  $t\bar{t}$  and  $b\bar{b}$  systems

$m_b \sim 5$  GeV       $t\bar{t}$  typical scale up to  $\sim 500$  GeV

scale choice and estimation of theoretical uncertainties non trivial

XS dominated by FS  $g \rightarrow b\bar{b}$  splittings  
[Ježo et al. '18]



it supports  
using  $m_b > 0$

# Discrepancies in $t\bar{t}b\bar{b}$ NLOPS generators

Standard factor-2  $\mu_R$  variations  $\sim 30\%$  NLO scale dependence

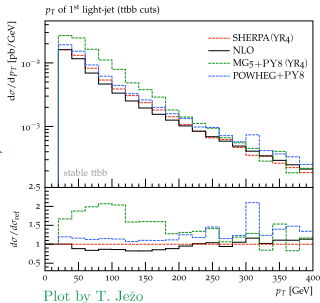
**But:** discrepancies between different NLOPS generators significantly exceed NLO scale variations

Most sensitive distribution: **light-jet  $p_T$  spectrum**  
up to 100% shape differences in the 100-200 GeV region

Most likely **hypothesis** on origin of NLOPS differences:  
interplay between PS and large NLO  $t\bar{t}b\bar{b}$   $K$ -factor  
 $\Rightarrow$  it enters the PS matching in the soft regime

**Idea:** reduce uncertainties discarding less accurate NLOPS predictions  
by means of a benchmark  $p_{T,j}$  with uncertainty well below 100%

Motivation for  $pp \rightarrow t\bar{t}b\bar{b}j$  at NLO QCD



origin of large  $K$ -factor  
to be understood

This talk

# Large NLO $K$ -factor

Input parameters, PDFs and scale choices [Ježo et al. '18]

$$m_b = 4.75 \text{ GeV}$$

$$m_t = 172.5 \text{ GeV}$$

$$\mu_R = \sqrt{\mu_{t\bar{t}}\mu_{b\bar{b}}} \quad \text{with} \quad \mu_{b\bar{b}} = \sqrt{E_{T,b}E_{T,\bar{b}}} \quad \mu_{t\bar{t}} = \sqrt{E_{T,t}E_{T,\bar{t}}} \quad \leftarrow \text{dynamic scales}$$

$$\mu_F = \frac{H_T}{2} = \frac{1}{2} \sum_{i=t,\bar{t},b,\bar{b},j} E_{T,i}$$

NLO PDFs are used throughout: both at LO and NLO

NNPDF\_nlo\_as\_0118\_nf\_4 with  $\alpha_s^{4f}$

# Large NLO $K$ -factor

Input parameters, PDFs and scale choices [Ježo et al. '18]

$$m_b = 4.75 \text{ GeV}$$

$$m_t = 172.5 \text{ GeV}$$

$$\mu_R = \sqrt{\mu_{t\bar{t}}\mu_{b\bar{b}}} \quad \text{with} \quad \mu_{b\bar{b}} = \sqrt{E_{T,b}E_{T,\bar{b}}} \quad \mu_{t\bar{t}} = \sqrt{E_{T,t}E_{T,\bar{t}}} \quad \leftarrow \text{dynamic scales}$$

$$\mu_F = \frac{H_T}{2} = \frac{1}{2} \sum_{i=t,\bar{t},b,\bar{b},j} E_{T,i}$$

NLO PDFs are used throughout: both at LO and NLO

NNPDF\_nlo\_as\_0118\_nf\_4 with  $\alpha_s^{4f}$

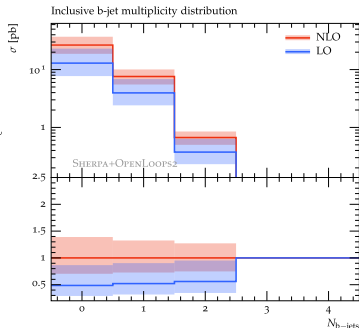
The NLO QCD cross sections for  $pp \rightarrow t\bar{t}b\bar{b}$  feature a **large  $K$ -factor**

**$K$ -factor**

$$N_{b\text{-jets} \geq 0} : 2.06$$

$$N_{b\text{-jets} \geq 1} : 1.92$$

$$N_{b\text{-jets} \geq 2} : 1.79$$



# Large NLO $K$ -factor

Input parameters, PDFs and scale choices [Ježo et al. '18]

$$m_b = 4.75 \text{ GeV}$$

$$m_t = 172.5 \text{ GeV}$$

$$\mu_R = \sqrt{\mu_{t\bar{t}}\mu_{b\bar{b}}} \quad \text{with} \quad \mu_{b\bar{b}} = \sqrt{E_{T,b}E_{T,\bar{b}}} \quad \mu_{t\bar{t}} = \sqrt{E_{T,t}E_{T,\bar{t}}} \quad \leftarrow \text{dynamic scales}$$

$$\mu_F = \frac{H_T}{2} = \frac{1}{2} \sum_{i=t,\bar{t},b,\bar{b},j} E_{T,i}$$

NLO PDFs are used throughout: both at LO and NLO

NNPDF\_nlo\_as\_0118\_nf\_4 with  $\alpha_s^{4f}$

The NLO QCD cross sections for  $pp \rightarrow t\bar{t}b\bar{b}$  feature a **large  $K$ -factor**

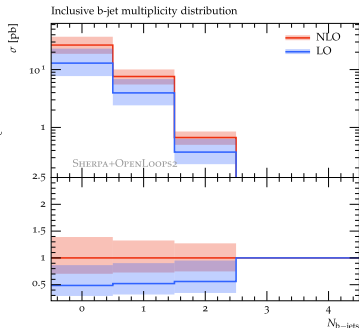
**$K$ -factor**

$$N_{b\text{-jets} \geq 0} : 2.06$$

$$N_{b\text{-jets} \geq 1} : 1.92$$

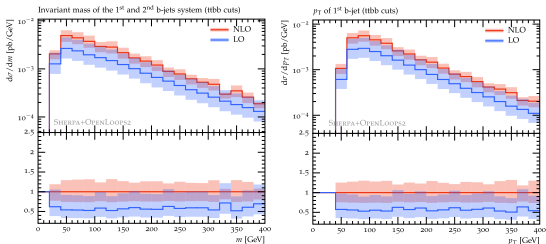
$$N_{b\text{-jets} \geq 2} : 1.79$$

more realistic picture of perturbative convergence but much bigger  $K$ -factor wrt using LO  $\alpha_s$  + PDFs for  $\sigma_{LO}$



# Large NLO $K$ -factor

$K$ -factor is large and stable for inclusive and exclusive observables



Such a large  $K$ -factor poses a question:

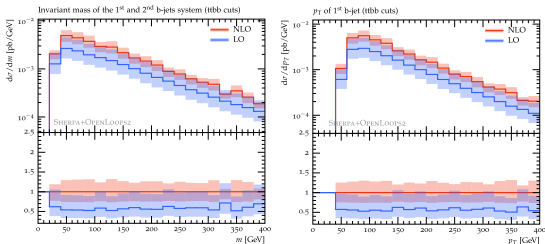
are corrections beyond NLO larger than factor 2 scale variations?



origin of large  $K$ -factor needs to be understood

# Large NLO $K$ -factor

$K$ -factor is large and stable for inclusive and exclusive observables



Such a large  $K$ -factor poses a question:

are corrections beyond NLO larger than factor 2 scale variations?



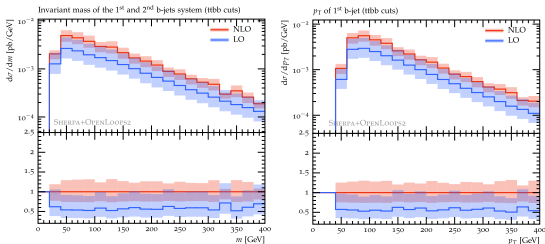
origin of large  $K$ -factor needs to be understood

Hypotheses on origin of large  $K$ -factor:



# Large NLO $K$ -factor

$K$ -factor is large and stable for inclusive and exclusive observables



Such a large  $K$ -factor poses a question:

are corrections beyond NLO larger than factor 2 scale variations?



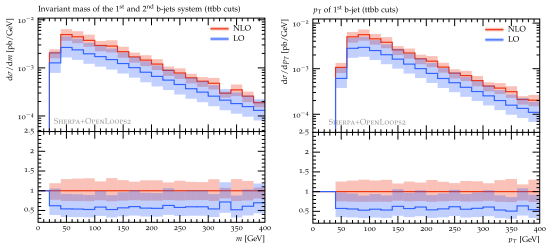
origin of large  $K$ -factor needs to be understood

Hypotheses on origin of large  $K$ -factor:

- (a) sizeable NLO real emission contribution  
large mass gap in  $t\bar{t}$  and  $b\bar{b}$  systems ( $m_b, p_{T,b} \ll m_t$ ),  
 $\sigma_{NLO}$  strongly enhanced by hard  $j$  radiation ( $m_t > p_{T,j} > p_{T,b}$ )

# Large NLO $K$ -factor

$K$ -factor is large and stable for inclusive and exclusive observables



Such a large  $K$ -factor poses a question:

are corrections beyond NLO larger than factor 2 scale variations?



origin of large  $K$ -factor needs to be understood

Hypotheses on origin of large  $K$ -factor:

- (a) **sizeable NLO real emission contribution**

large mass gap in  $t\bar{t}$  and  $b\bar{b}$  systems ( $m_b, p_{T,b} \ll m_t$ ),

$\sigma_{NLO}$  strongly enhanced by hard  $j$  radiation ( $m_t > p_{T,j} > p_{T,b}$ )

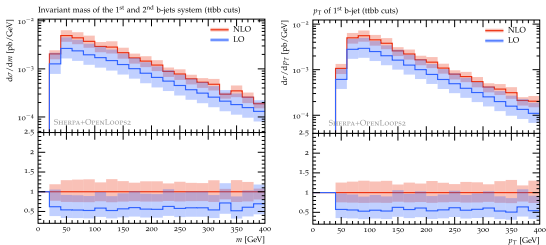
may be interpreted as  $t\bar{t}g\bar{g}(g \rightarrow b\bar{b})$

↓  
described at LO

↓  
potentially large corrections beyond NLO

# Large NLO $K$ -factor

$K$ -factor is large and stable for inclusive and exclusive observables



Such a large  $K$ -factor poses a question:

are corrections beyond NLO larger than factor 2 scale variations?



origin of large  $K$ -factor needs to be understood

Hypotheses on origin of large  $K$ -factor:

- (a) sizeable NLO real emission contribution  
large mass gap in  $t\bar{t}$  and  $b\bar{b}$  systems ( $m_b, p_{T,b} \ll m_t$ ),  
 $\sigma_{NLO}$  strongly enhanced by hard  $j$  radiation ( $m_t > p_{T,j} > p_{T,b}$ )
- (b) a non-optimal  $\mu_R$  scale choice

may be interpreted as  $t\bar{t}g\bar{g}(g \rightarrow b\bar{b})$

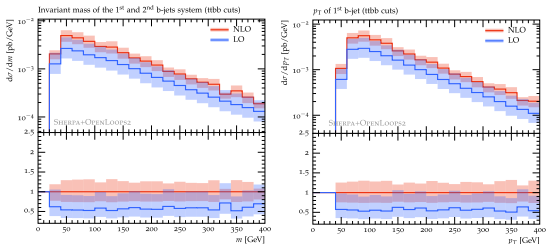
described at LO



potentially large corrections beyond NLO

# Large NLO $K$ -factor

$K$ -factor is large and stable for inclusive and exclusive observables



Such a large  $K$ -factor poses a question:

are corrections beyond NLO larger than factor 2 scale variations?



origin of large  $K$ -factor needs to be understood

Hypotheses on origin of large  $K$ -factor:

- (a) **sizeable NLO real emission contribution**  
large mass gap in  $t\bar{t}$  and  $b\bar{b}$  systems ( $m_b, p_{T,b} \ll m_t$ ),  
 $\sigma_{NLO}$  strongly enhanced by hard  $j$  radiation ( $m_t > p_{T,j} > p_{T,b}$ )
- (b) a **non-optimal  $\mu_R$  scale choice**

may be interpreted as  $t\bar{t}g\bar{g}(g \rightarrow b\bar{b})$

described at LO



potentially large corrections beyond NLO

a more appropriate  $\mu_R$  choice might reduce the  $K$ -factor and also mitigate the NLOPS discrepancies

# Mass effects on $pp \rightarrow t\bar{t}b\bar{b}$ cross sections

**Aim:** try to understand if the large  $K$ -factor is related to  $m_t \gg m_b$

**Idea:** study the behaviour of the NLO  $K$ -factor for different mass configurations using an “interpolating” mass  $m^* = \sqrt{m_b m_t} \sim 28.62$  GeV

masses [GeV]		$\sigma_{N_{b\text{-jet}} \geq 0}$ [pb]			$\sigma_{N_{b\text{-jet}} \geq 1}$ [pb]			$\sigma_{N_{b\text{-jet}} \geq 2}$ [pb]		
$m_b$	$m_t$	LO	NLO	$\frac{\text{NLO}}{\text{LO}}$	LO	NLO	$\frac{\text{NLO}}{\text{LO}}$	LO	NLO	$\frac{\text{NLO}}{\text{LO}}$
4.75	172.5	12.94	26.61	2.06	3.955	7.593	1.92	0.374	0.669	1.79
28.62	28.62	321.1	642.4	2.0	165.3	317.7	1.92	34.61	63.42	1.83
28.62	172.5	0.999	1.911	1.9	0.752	1.400	1.86	0.245	0.437	1.78
172.5	172.5	0.013	0.023	1.82	0.013	0.023	1.81	$9.31 \cdot 10^{-3}$	$1.67 \cdot 10^{-2}$	1.79

Dynamic scales choice:

$$\mu_R = \prod_{i=t,\bar{t},b,\bar{b}} E_{T,i}^{1/4}$$

$$\mu_F = \frac{H_T}{2}$$

# Mass effects on $pp \rightarrow t\bar{t}b\bar{b}$ cross sections

**Aim:** try to understand if the large  $K$ -factor is related to  $m_t \gg m_b$

**Idea:** study the behaviour of the NLO  $K$ -factor for different mass configurations using an “interpolating” mass  $m^* = \sqrt{m_b m_t} \sim 28.62$  GeV

masses [GeV]		$\sigma_{N_{b\text{-jets}} \geq 0}$ [pb]			$\sigma_{N_{b\text{-jets}} \geq 1}$ [pb]			$\sigma_{N_{b\text{-jets}} \geq 2}$ [pb]		
$m_b$	$m_t$	LO	NLO	$\frac{\text{NLO}}{\text{LO}}$	LO	NLO	$\frac{\text{NLO}}{\text{LO}}$	LO	NLO	$\frac{\text{NLO}}{\text{LO}}$
4.75	172.5	12.94	26.61	2.06	3.955	7.593	1.92	0.374	0.669	1.79
28.62	28.62	321.1	642.4	2.0	165.3	317.7	1.92	34.61	63.42	1.83
28.62	172.5	0.999	1.911	1.9	0.752	1.400	1.86	0.245	0.437	1.78
172.5	172.5	0.013	0.023	1.82	0.013	0.023	1.81	$9.31 \cdot 10^{-3}$	$1.67 \cdot 10^{-2}$	1.79

Dynamic scales choice:

$$\mu_R = \prod_{i=t,\bar{t},b,\bar{b}} E_{T,i}^{1/4}$$

$$\mu_F = \frac{H_T}{2}$$

× Large  $K$ -factor stable  
 wrt variations of  $m_t$ ,  $m_b$  gap  
 ⇒ hypothesis (a) disfavoured

# Mass effects on $pp \rightarrow t\bar{t}b\bar{b}$ cross sections

**Aim:** try to understand if the large  $K$ -factor is related to  $m_t \gg m_b$

**Idea:** study the behaviour of the NLO  $K$ -factor for different mass configurations using an “interpolating” mass  $m^* = \sqrt{m_b m_t} \sim 28.62$  GeV

masses [GeV]		$\sigma_{N_{b\text{-jet}\geq 0}$ [pb]			$\sigma_{N_{b\text{-jet}\geq 1}$ [pb]			$\sigma_{N_{b\text{-jet}\geq 2}$ [pb]		
$m_b$	$m_t$	LO	NLO	$\frac{\text{NLO}}{\text{LO}}$	LO	NLO	$\frac{\text{NLO}}{\text{LO}}$	LO	NLO	$\frac{\text{NLO}}{\text{LO}}$
4.75	172.5	12.94	26.61	2.06	3.955	7.593	1.92	0.374	0.669	1.79
28.62	28.62	321.1	642.4	2.0	165.3	317.7	1.92	34.61	63.42	1.83
28.62	172.5	0.999	1.911	1.9	0.752	1.400	1.86	0.245	0.437	1.78
172.5	172.5	0.013	0.023	1.82	0.013	0.023	1.81	$9.31 \cdot 10^{-3}$	$1.67 \cdot 10^{-2}$	1.79

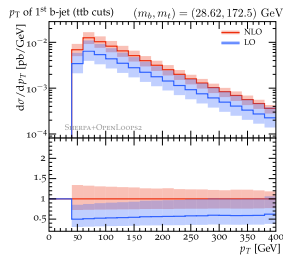
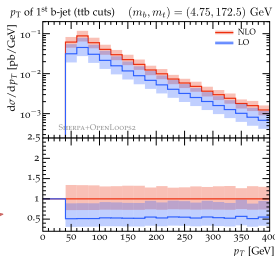
Dynamic scales choice:

$$\mu_R = \prod_{i=t,\bar{t},b,\bar{b}} E_{T,i}^{1/4}$$

$$\mu_F = \frac{H_T}{2}$$

× Large  $K$ -factor stable wrt variations of  $m_t, m_b$  gap  $\Rightarrow$  hypothesis (a) disfavoured

✓ good shapes in distributions



# Fixed vs dynamic $\mu_R$ scale choice

If no mass gap i.e.  $m_b = m_t$  there would be a natural choice  $\Rightarrow \mu_R = m_t$

A direct generalization could be  $\mu_R = \sqrt{m_b m_t}$   $\longrightarrow$  moderate  $K$ -factor for different  $m_b, m_t$



# Fixed vs dynamic $\mu_R$ scale choice

If no mass gap i.e.  $m_b = m_t$  there would be a natural choice  $\Rightarrow \mu_R = m_t$

A direct generalization could be  $\mu_R = \sqrt{m_b m_t} \longrightarrow$  moderate  $K$ -factor for different  $m_b, m_t$

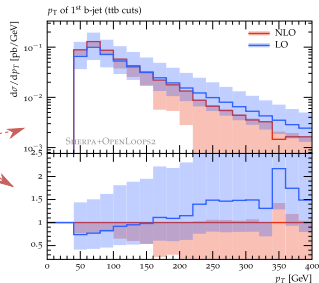
Physical case:  $m_b = 4.75$  GeV,  $m_t = 172.5$  GeV

$\sqrt{m_b m_t} \sim 28.62$  GeV and  $K$ -factor  $\sim 1.47$

✓ reduced  $K$ -factor

✗ enhanced shape distortion in distributions

✗ unreliable scale uncertainties



# Fixed vs dynamic $\mu_R$ scale choice

If no mass gap i.e.  $m_b = m_t$  there would be a natural choice  $\Rightarrow \mu_R = m_t$

A direct generalization could be  $\mu_R = \sqrt{m_b m_t} \longrightarrow$  moderate  $K$ -factor for different  $m_b, m_t$

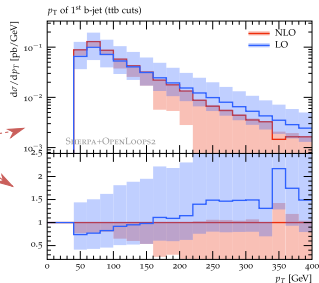
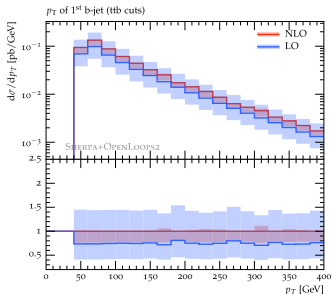
Physical case:  $m_b = 4.75$  GeV,  $m_t = 172.5$  GeV

$\sqrt{m_b m_t} \sim 28.62$  GeV and  $K$ -factor  $\sim 1.47$

✓ reduced  $K$ -factor

✗ enhanced shape distortion in distributions

✗ unreliable scale uncertainties



motivates a reduced dynamic  $\mu_R$

Example: factor 3 reduction of  $\mu_R$

✓ reduced  $K$ -factor

✓ no shape distortions in distributions

✓  $\sim 20\%$  scale uncertainties

# Renormalisation scale dependence

Both at LO and NLO **scale uncertainties** are **dominated by  $\mu_R$**  variations.

Default choice of scale:  $\mu_R = \mu_{def} \equiv \prod_{i=t,\bar{t},b,\bar{b}} E_{T,i}^{1/4}$

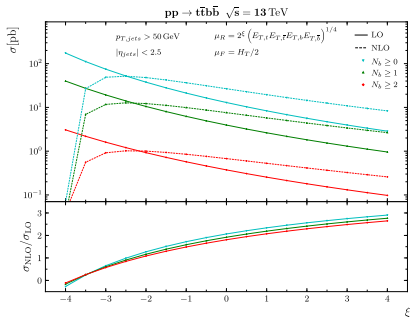
Average value  $\bar{\mu}_{def} \Rightarrow N_{b \geq 0} \sim 73 \text{ GeV} \quad N_{b \geq 1} \sim 93 \text{ GeV} \quad N_{b \geq 2} \sim 124 \text{ GeV}$

# Renormalisation scale dependence

Both at LO and NLO **scale uncertainties** are **dominated by  $\mu_R$**  variations.

Default choice of scale:  $\mu_R = \mu_{def} \equiv \prod_{i=t,\bar{t},b,\bar{b}} E_{T,i}^{1/4}$

Average value  $\bar{\mu}_{def} \Rightarrow N_{b \geq 0} \sim 73 \text{ GeV} \quad N_{b \geq 1} \sim 93 \text{ GeV} \quad N_{b \geq 2} \sim 124 \text{ GeV}$



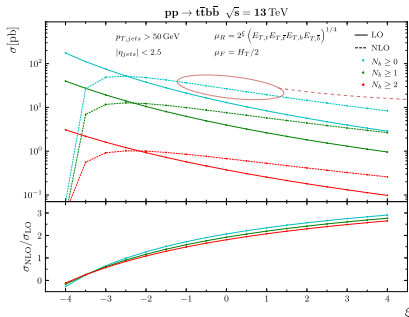
$$\mu_R = 2^\xi (E_{T,t} E_{T,\bar{t}} E_{T,b} E_{T,\bar{b}})^{1/4}$$

# Renormalisation scale dependence

Both at LO and NLO **scale uncertainties** are **dominated by  $\mu_R$**  variations.

Default choice of scale:  $\mu_R = \mu_{def} \equiv \prod_{i=t,\bar{t},b,\bar{b}} E_{T,i}^{1/4}$

Average value  $\bar{\mu}_{def} \Rightarrow N_{b \geq 0} \sim 73 \text{ GeV} \quad N_{b \geq 1} \sim 93 \text{ GeV} \quad N_{b \geq 2} \sim 124 \text{ GeV}$



$\mu_R = 2^\xi (E_{T,t} E_{T,\bar{t}} E_{T,b} E_{T,\bar{b}})^{1/4}$

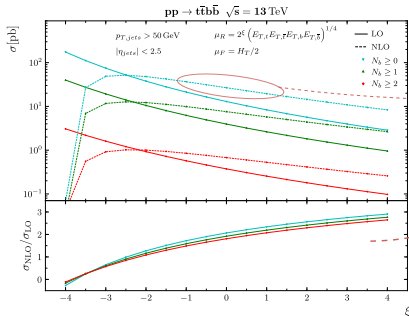
factor 2 variation:  $\sim 27\%$  NLO uncertainty

# Renormalisation scale dependence

Both at LO and NLO **scale uncertainties** are **dominated by  $\mu_R$**  variations.

Default choice of scale:  $\mu_R = \mu_{def} \equiv \prod_{i=t,\bar{t},b,\bar{b}} E_{T,i}^{1/4}$

Average value  $\bar{\mu}_{def} \Rightarrow N_{b \geq 0} \sim 73 \text{ GeV} \quad N_{b \geq 1} \sim 93 \text{ GeV} \quad N_{b \geq 2} \sim 124 \text{ GeV}$



$\mu_R = 2^\xi (E_{T,t} E_{T,\bar{t}} E_{T,b} E_{T,\bar{b}})^{1/4}$

factor 2 variation:  $\sim 27\%$  NLO uncertainty

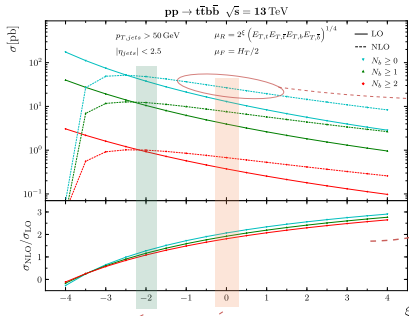
similar  $K$ -factor for different  $b$ -jets multiplicities

# Renormalisation scale dependence

Both at LO and NLO **scale uncertainties** are **dominated by  $\mu_R$**  variations.

Default choice of scale:  $\mu_R = \mu_{def} \equiv \prod_{i=t,\bar{t},b,\bar{b}} E_{T,i}^{1/4}$

Average value  $\bar{\mu}_{def} \Rightarrow N_{b \geq 0} \sim 73 \text{ GeV} \quad N_{b \geq 1} \sim 93 \text{ GeV} \quad N_{b \geq 2} \sim 124 \text{ GeV}$



$$\mu_R = 2^\xi (E_{T,t} E_{T,\bar{t}} E_{T,b} E_{T,\bar{b}})^{1/4}$$

factor 2 variation:  $\sim 27\%$  NLO uncertainty

similar  $K$ -factor for different  $b$ -jets multiplicities

default

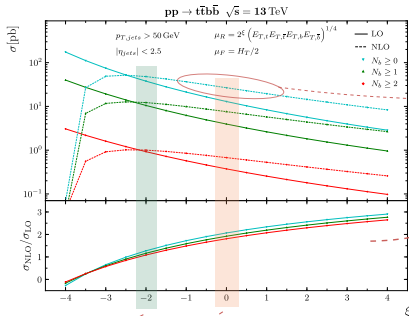
region where  $K$ -factor  $\sim 1$ , close the maximum of the NLO XS

# Renormalisation scale dependence

Both at LO and NLO **scale uncertainties** are **dominated by  $\mu_R$**  variations.

Default choice of scale:  $\mu_R = \mu_{def} \equiv \prod_{i=t,\bar{t},b,\bar{b}} E_{T,i}^{1/4}$

Average value  $\bar{\mu}_{def} \Rightarrow N_{b \geq 0} \sim 73 \text{ GeV} \quad N_{b \geq 1} \sim 93 \text{ GeV} \quad N_{b \geq 2} \sim 124 \text{ GeV}$



$$\mu_R = 2^\xi (E_{T,t} E_{T,\bar{t}} E_{T,b} E_{T,\bar{b}})^{1/4}$$

factor 2 variation:  $\sim 27\%$  NLO uncertainty

similar  $K$ -factor for different  $b$ -jets multiplicities

a factor 2-4 reduction of  $\mu_R$  brings  $K$ -factor close to 1 and scale uncertainty  $\sim 20\%$

default

region where  $K$ -factor  $\sim 1$ , close the maximum of the NLO XS

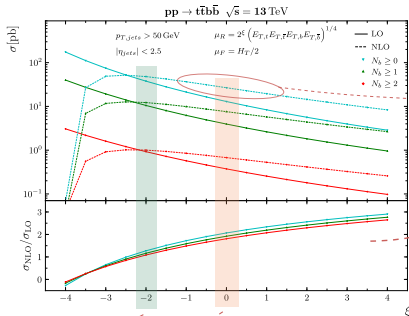


# Renormalisation scale dependence

Both at LO and NLO **scale uncertainties** are **dominated by  $\mu_R$**  variations.

Default choice of scale:  $\mu_R = \mu_{def} \equiv \prod_{i=t,\bar{t},b,\bar{b}} E_{T,i}^{1/4}$

Average value  $\bar{\mu}_{def} \Rightarrow N_{b \geq 0} \sim 73 \text{ GeV} \quad N_{b \geq 1} \sim 93 \text{ GeV} \quad N_{b \geq 2} \sim 124 \text{ GeV}$



$$\mu_R = 2^\xi (E_{T,t} E_{T,\bar{t}} E_{T,b} E_{T,\bar{b}})^{1/4}$$

factor 2 variation:  $\sim 27\%$  NLO uncertainty

similar  $K$ -factor for different  $b$ -jets multiplicities

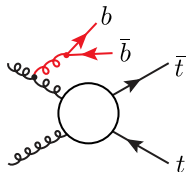
a factor 2-4 reduction of  $\mu_R$  brings  $K$ -factor close to 1 and scale uncertainty  $\sim 20\%$

default

region where  $K$ -factor  $\sim 1$ , close the maximum of the NLO XS

it seems to support hypothesis (b)

# Alternative $\mu_R$ choice



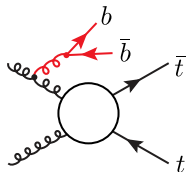
Alternative  $\mu_R$  based on  $k_T$  of splittings in dominant  $t\bar{t}b\bar{b}$  topologies

$$\mu_R = \mu_{gbb} \equiv (E_{T,t} E_{T,\bar{t}} E_{T,b\bar{b}} m_{b\bar{b}})^{1/4}$$

In general it is a **harder scale** than  $\mu_{def}$ :  $\bar{\mu}_{gbb} \sim 125$  GeV  $\bar{\mu}_{def} \sim 93$  GeV

↳ hence a larger  $K$ -factor than  $\mu_{def}$  at central value

# Alternative $\mu_R$ choice



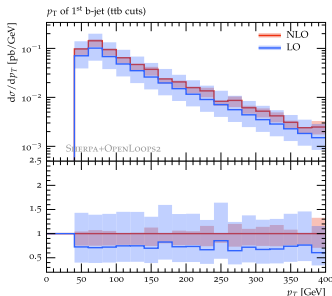
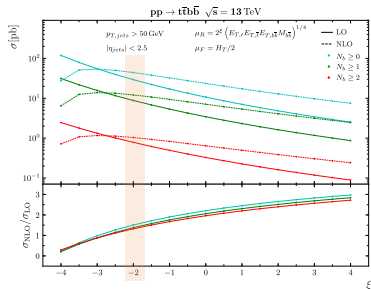
Alternative  $\mu_R$  based on  $k_T$  of splittings in dominant  $t\bar{t}b\bar{b}$  topologies

$$\mu_R = \mu_{gbb} \equiv (E_{T,t} E_{T,\bar{t}} E_{T,b\bar{b}} m_{b\bar{b}})^{1/4}$$

In general it is a **harder scale** than  $\mu_{def}$ :  $\bar{\mu}_{gbb} \sim 125$  GeV  $\bar{\mu}_{def} \sim 93$  GeV

↳ hence a larger  $K$ -factor than  $\mu_{def}$  at central value

Example:  $\frac{\mu_{gbb}}{4} \Rightarrow K\text{-factor} \sim 1.4$  yields 20-25% scale uncertainty at NLO



✓ good shape of  $K$ -factor for relevant distributions

# $pp \rightarrow t\bar{t}b\bar{b}j$ at NLO QCD

**Disclaimer:** all results are preliminary!

# $pp \rightarrow t\bar{t}b\bar{b}j$ at NLO QCD

**Disclaimer:** all results are preliminary!

First jet emission from matrix element  $\Rightarrow$  accurate benchmark for  $p_T$  of light jet radiation

# $pp \rightarrow t\bar{t}b\bar{b}j$ at NLO QCD

**Disclaimer:** all results are preliminary!

First jet emission from matrix element  $\Rightarrow$  accurate benchmark for  $p_T$  of light jet radiation

We consider  $pp \rightarrow t\bar{t}b\bar{b}j$  at 13 TeV centre of mass energy

- ▷ top quark stable, not decayed
- ▷ jets reconstructed using anti- $k_T$  algorithm  
as implemented in `FastJet-3.2`
- ▷  $\Delta R = 0.4$ ,  $p_T > 50$  GeV,  $|\eta| < 2.5$
- ▷ input parameters and scales choice  
choice as in  $t\bar{t}b\bar{b}$

# $pp \rightarrow t\bar{t}b\bar{b}j$ at NLO QCD

**Disclaimer:** all results are preliminary!

First jet emission from matrix element  $\Rightarrow$  accurate benchmark for  $p_T$  of light jet radiation

We consider  $pp \rightarrow t\bar{t}b\bar{b}j$  at 13 TeV centre of mass energy

- ▷ top quark stable, not decayed
- ▷ jets reconstructed using anti- $k_T$  algorithm  
as implemented in FastJet-3.2
- ▷  $\Delta R = 0.4$ ,  $p_T > 50$  GeV,  $|\eta| < 2.5$
- ▷ input parameters and scales choice  
choice as in  $t\bar{t}b\bar{b}$

*b*-jets tagging

“single-tagged”:  $b$  or  $\bar{b}$  quark content

“double-tagged”:  $b\bar{b}$  content

generic  $b$ -jet:  $b$ ,  $\bar{b}$  and  $b\bar{b}$  equally counted

this talk

important for comparisons against PS

# OpenLoops2 for $t\bar{t}b\bar{b}j$ 1-loop MEs

The 1-loop matrix elements relevant for  $t\bar{t}b\bar{b}$  and  $t\bar{t}b\bar{b}j$  production are computed using

OpenLoops2: new on-the-fly helicity summation and integrand reduction [F.B., S.Pozzorini, M.Zoller '17]

The full hadronic prediction is provided through OpenLoops2 + SHERPA-2.2.4

see talk from Max Zoller



same interface as OL1





# OpenLoops2 for $t\bar{t}b\bar{b}j$ 1-loop MEs

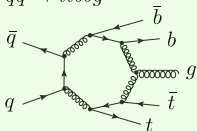
The 1-loop matrix elements relevant for  $t\bar{t}b\bar{b}$  and  $t\bar{t}b\bar{b}j$  production are computed using

**OpenLoops2: new on-the-fly helicity summation and integrand reduction** [F.B., S.Pozzorini, M.Zoller '17]

The full hadronic prediction is provided through **OpenLoops2 + SHERPA-2.2.4** see talk from Max Zoller

In the 4F scheme there are two main partonic channels (+ crossings): same interface as OL1

$$q\bar{q} \rightarrow t\bar{t}b\bar{b}g$$

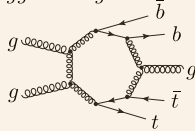


- up to rank 4  
7-point 1-loop integrals
- 3534 1L Feyn. diags.
- $2^6$  relevant helicity configurations

**Timings**[s/point] (colour + helicity sums)

	OL1	OL2+Collier	OL2+OFR
$m_b = 0$	0.337	0.208	0.233
$m_b \neq 0$	0.593	0.269	0.297

$$gg \rightarrow t\bar{t}b\bar{b}g$$



- up to rank 5  
7-point 1-loop integrals
- 25431 1L Feyn. diags.
- $2^7$  relevant helicity configurations

**Timings**[s/point]

	OL1	OL2+Collier	OL2+OFR
$m_b = 0$	4.671	1.877	2.141
$m_b \neq 0$	8.706	2.650	2.958

# OpenLoops2 for $t\bar{t}b\bar{b}j$ 1-loop MEs

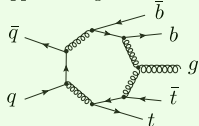
The 1-loop matrix elements relevant for  $t\bar{t}b\bar{b}$  and  $t\bar{t}b\bar{b}j$  production are computed using

**OpenLoops2: new on-the-fly helicity summation and integrand reduction** [F.B., S.Pozzorini, M.Zoller '17]

The full hadronic prediction is provided through **OpenLoops2 + SHERPA-2.2.4** see talk from Max Zoller

In the 4F scheme there are two main partonic channels (+ crossings): same interface as OL1

$$q\bar{q} \rightarrow t\bar{t}b\bar{b}g$$

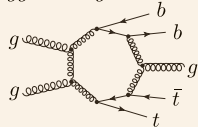


- up to rank 4  
7-point 1-loop integrals
- 3534 1L Feyn. diags.
- $2^6$  relevant helicity configurations

**Timings**[s/point] (colour + helicity sums)

	OL1	OL2+Collier	OL2+OFR
$m_b = 0$	0.337	0.208	0.233
$m_b \neq 0$	0.593	0.269	0.297

$$gg \rightarrow t\bar{t}b\bar{b}g$$



- up to rank 5  
7-point 1-loop integrals
- 25431 1L Feyn. diags.
- $2^7$  relevant helicity configurations

**Timings**[s/point]

	OL1	OL2+Collier	OL2+OFR
$m_b = 0$	4.671	1.877	2.141
$m_b \neq 0$	8.706	2.650	2.958

+75 - 85%

~ +40%

OL1/OL2 up to 3!

# SHERPA + OpenLoops2

$$\sigma_n^{\text{NLO}} = \int d\Phi_n [\mathcal{B}(\Phi_n) + \mathcal{V}(\Phi_n)] + \int d\Phi_{n+1} \mathcal{R}(\Phi_{n+1})$$

Dipole subtraction method [Catani, Seymour '96]: **factorisation** and **universality** of IR singularities

$$\mathcal{R}(\Phi_{n+1}) \rightarrow \mathcal{B} \otimes \mathcal{S}(\Phi_1) \quad \mathcal{I} = \int d\Phi_1 \mathcal{S}(\Phi_1) \Rightarrow \text{integrated analytically}$$

It allows for an IR safe numerical integration of the cross section

$$\sigma_n^{\text{NLO}} = \int d\Phi_n [\mathcal{B}(\Phi_n) + \mathcal{V}(\Phi_n) + \mathcal{B}(\Phi_n) \otimes \mathcal{I}] + \int d\Phi_{n+1} [\mathcal{R}(\Phi_{n+1}) - \mathcal{B}(\Phi_n) \otimes \mathcal{S}(\Phi_1)]$$

# SHERPA + OpenLoops2

$$\sigma_n^{\text{NLO}} = \int d\Phi_n [\mathcal{B}(\Phi_n) + \mathcal{V}(\Phi_n)] + \int d\Phi_{n+1} \mathcal{R}(\Phi_{n+1})$$

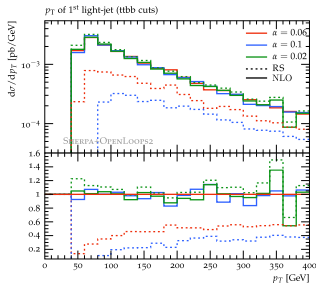
Dipole subtraction method [Catani, Seymour '96]: **factorisation** and **universality** of IR singularities

$$\mathcal{R}(\Phi_{n+1}) \rightarrow \mathcal{B} \otimes \mathcal{S}(\Phi_1) \quad \mathcal{I} = \int d\Phi_1 \mathcal{S}(\Phi_1) \Rightarrow \text{integrated analytically}$$

It allows for an IR safe numerical integration of the cross section

$$\sigma_n^{\text{NLO}} = \int d\Phi_n [\mathcal{B}(\Phi_n) + \mathcal{V}(\Phi_n) + \mathcal{B}(\Phi_n) \otimes \mathcal{I}] + \int d\Phi_{n+1} [\mathcal{R}(\Phi_{n+1}) - \mathcal{B}(\Phi_n) \otimes \mathcal{S}(\Phi_1)]$$

In Sherpa the dipole phase space can be restricted by means of DIPOLE\_ALPHA



Varying  $\alpha$  offers a check of the consistency of the subtraction

first validation of the calculation ✓

$\alpha$	NLO[pb]	BVI[pb]	RS[pb]
0.02	$3.253 \cdot 10^{-1}$	$-0.32 \cdot 10^{-1}$	$3.57 \cdot 10^{-1}$
0.06	$3.266 \cdot 10^{-1}$	$1.97 \cdot 10^{-1}$	$1.30 \cdot 10^{-1}$
0.1	$3.247 \cdot 10^{-1}$	$2.73 \cdot 10^{-1}$	$0.52 \cdot 10^{-1}$

$N_{b\text{-jets} \geq 2}$  XS

# $pp \rightarrow t\bar{t}b\bar{b}j$ cross sections at 13 TeV

Process	$\sigma_{N_{b\text{-jets}} \geq 1}$ [pb]			$\sigma_{N_{t\text{-jets}} \geq 2}$ [pb]		
	LO	NLO	$\frac{\text{NLO}}{\text{LO}}$	LO	NLO	$\frac{\text{NLO}}{\text{LO}}$
$t\bar{t}b\bar{b}, \mu_{def}$	3.955 <sup>+73%</sup> <sub>-39%</sub>	7.593 <sup>+32%</sup> <sub>-27%</sub>	1.92	0.374 <sup>+69%</sup> <sub>-38%</sub>	0.669 <sup>+27%</sup> <sub>-25%</sub>	1.79
$t\bar{t}b\bar{b}, \mu_{gbb}$	3.441 <sup>+70%</sup> <sub>-38%</sub>	7.089 <sup>+37%</sup> <sub>-28%</sub>	2.06	0.327 <sup>+67%</sup> <sub>-37%</sub>	0.642 <sup>+33%</sup> <sub>-27%</sub>	1.96
$t\bar{t}b\bar{b}j, \mu_{def}$	2.164 <sup>+96%</sup> <sub>-45%</sub>	3.670 <sup>+27%</sup> <sub>-30%</sub>	1.70	0.219 <sup>+90%</sup> <sub>-44%</sub>	0.327 <sup>+12%</sup> <sub>-25%</sub>	1.49
$t\bar{t}b\bar{b}j, \mu_{gbb}$	1.894 <sup>+93%</sup> <sub>-45%</sub>	4.120 <sup>+46%</sup> <sub>-34%</sub>	2.17	0.188 <sup>+87%</sup> <sub>-43%</sub>	0.354 <sup>+36%</sup> <sub>-30%</sub>	1.88

▷ Scale uncertainty dominated by  $\mu_R$  variations (as in  $t\bar{t}b\bar{b}$ )

▷ For  $pp \rightarrow t\bar{t}b\bar{b}j$   $\sigma_{LO} \propto \alpha_s^5$   
up to  $\sim 90 - 95\%$  scale uncertainty

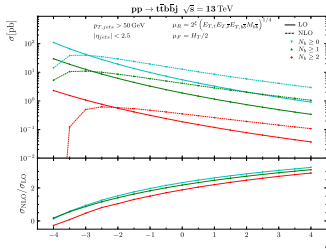
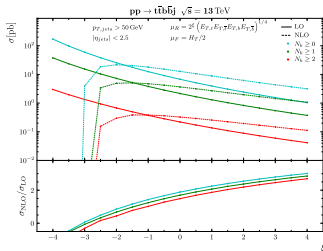
**K-factor:**

▷ slightly smaller wrt  $t\bar{t}b\bar{b}$

but still significant

▷ quite large for  $\mu_{gbb}$   
bit smaller for  $\mu_{def}$

▷ can be reduced by  
rescaling the central  
value



# $b$ -jets distributions

We consider the phase space with two resolved  $b$ -jets

## $K$ -factor

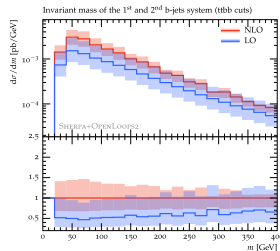
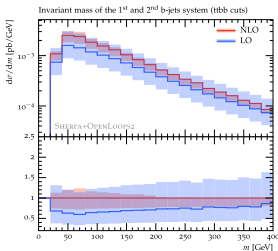
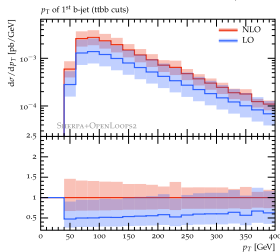
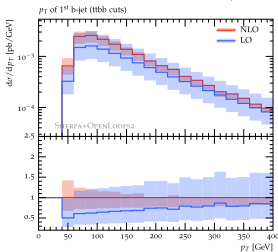
- ▶ quite stable for both scale choices
- ▶ though **more stable** for  $\mu_{gbb}$  over the full spectrum

## Scale uncertainty at NLO

- ▶ compatible with uncertainty on the cross section:
  - ranges in  $\sim 10$ -25% for  $\mu_{def}$
  - lives around 35% for  $\mu_{gbb}$
- ▶ for both scale choices, the uncertainty reduces in the tails
- ▶  $\mu_{def}$  shows a smaller scale uncertainty overall  
 due to  $\bar{\mu}_{def} < \bar{\mu}_{gbb}$

$$\mu_R = \mu_{def} \downarrow$$

$$\mu_R = \mu_{gbb} \downarrow$$



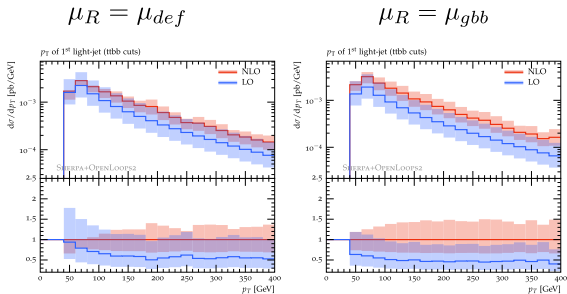
# Light-jet $p_T$ spectrum at NLO

## $K$ -factor

- ▶ significant shape distortions for  $\mu_{def}$  below 100-200 GeV
- ▶ more stable for  $\mu_{gbb}$

## Scale uncertainty at NLO

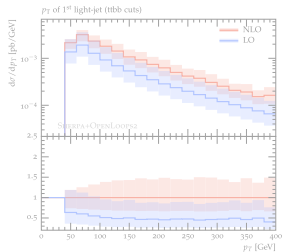
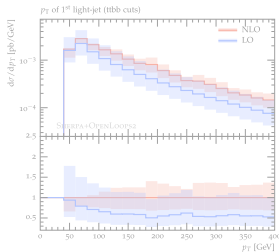
- ▶ contrary to  $b$ -jet distribution it increases in the tail
- ▶ up to 40%-50%



# Light-jet $p_T$ spectrum at NLO

$$\mu_R = \mu_{def}^j$$

$$\mu_R = \mu_{gbb}^j$$

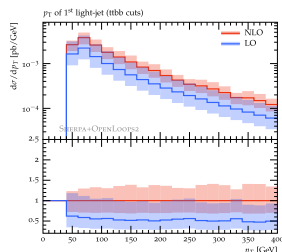
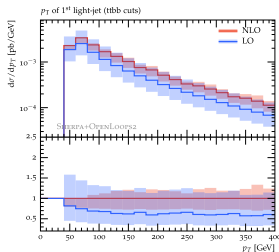


Scale choices which include jet  $p_T$

$$\mu_{def}^j = (E_{T,t} E_{T,\bar{t}} E_{T,b} E_{T,\bar{b}} p_{T,j})^{1/5}$$

$$\mu_{gbb}^j = (E_{T,t} E_{T,\bar{t}} M_{T,b\bar{b}} E_{T,b\bar{b}} p_{T,j})^{1/5}$$

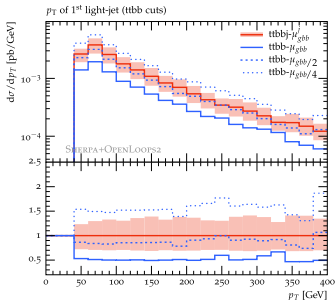
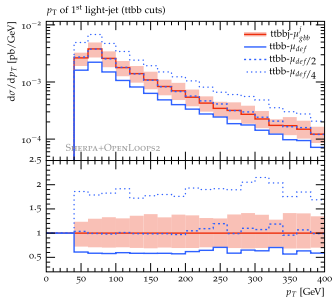
tends to reduce NLO uncertainties  
and shape distortions  
especially with  $\mu_{gbb}$





# $t\bar{t}b\bar{b}$ vs $t\bar{t}b\bar{b}j$ NLO predictions for $p_{T,j}$

Reference scale choice:  $\mu_R = \mu_{gbb}^j \equiv (E_{T,t}E_{T,\bar{t}}m_{b\bar{b}}E_{T,b\bar{b}}p_{T,j})^{1/5}$



✓ remarkably good shape agreement over all the  $p_T$  spectrum

✓ rescaling  $\mu_{gbb}$  by 0.5 in  $t\bar{t}b\bar{b}$   
 $\sim 15\%$  agreement with NLO  $t\bar{t}b\bar{b}j$

✓ rescaling  $\mu_{def}$  by 0.5 in  $t\bar{t}b\bar{b}$   
 $\rightarrow$  within few % agreement with NLO  $t\bar{t}b\bar{b}j$

benchmark with precision of  $\sim 30\%$   
to select optimal  $t\bar{t}b\bar{b}$  scale

it motivates reduction of conventional  $t\bar{t}b\bar{b}$   
by a factor 2 (or more)

consistent with arguments based on  
reduction of inclusive  $t\bar{t}b\bar{b}$   $K$ -factor

# Summary

- ▶  $t\bar{t}H(H \rightarrow b\bar{b})$  searches limited by theoretical uncertainty on  $t\bar{t} + b$ -jets background
- ▶ crucial to understand sizeable discrepancies between NLOPS  $t\bar{t}b\bar{b}$  MC on the market
  - most notably in the spectrum of extra light-jet radiation
  - related to large  $t\bar{t}b\bar{b}$  NLO  $K$ -factor
- ▶ We have shown that the scale dependence of  $\sigma_{t\bar{t}b\bar{b}}$  and its interplay with the  $m_t/m_b$  mass gap support a reduced  $\mu_R$  choice, which would:
  - yield a smaller  $K$ -factor and a smaller scale uncertainty
  - probably mitigate NLOPS discrepancies
- ▶ We have presented NLO predictions for  $pp \rightarrow t\bar{t}b\bar{b}j$ 
  - first application of `OpenLoops2` (with `SHERPA`)
  - provides additional support for using a reduced  $\mu_R$  choice in  $pp \rightarrow t\bar{t}b\bar{b}$
  - should help reducing NLOPS uncertainties  
(by discarding less accurate MC predictions for light-jet spectrum)